

## Peak Temperatures of Large Solar X-ray Events and Associated CME Speeds

---

**S. W. Kahler\***

*Air Force Research Laboratory, Space Vehicles Directorate, Kirtland AFB, NM, USA*  
stephen.kahler@us.af.mil

**A. G. Ling**

*Atmospheric Environmental Research, Albuquerque, NM, USA*

Recently we [1] repeated an earlier analysis by [2,3] showing that large ( $> M3$ ) solar X-ray flares associated with solar energetic particle (SEP) events have significantly lower peak X-ray flux ratios  $R$  of 0.04-0.5/0.1-0.8 nm, proxies for flare peak temperatures, than those without SEP events. Since we expect SEP events to be produced by shocks ahead of fast coronal mass ejections (CMEs), this would imply that an X-ray flare of a given peak flux is more likely to have a fast CME and associated SEP event when it has a relatively smaller  $R$ . We examine the role played by the ratios  $R$  in correlations between X-ray peak flare fluxes and CME speeds  $V_{cme}$ , and then compare CMEs widths  $W$ , speeds  $V_{cme}$ , X-ray flare durations  $\Delta T$ , and  $R$  with each other. We resolve the apparent conflict between a global scaling model of eruptive events showing  $V_{cme}$  scaling with higher  $R$  and our confirmation that the [2,3] analysis implies faster CMEs are associated with flares of lower  $R$ .

*36th International Cosmic Ray Conference -ICRC2019-  
July 24th - August 1st, 2019  
Madison, WI, U.S.A.*

---

\*Speaker.

## 1. Introduction

Large solar energetic ( $E > 10$  MeV) particle (SEP) events are understood to be produced in coronal shocks driven by fast ( $V_{cme} \geq 900$  km s<sup>-1</sup>) coronal mass ejections (CMEs) [4,5,6]. Those CMEs are nearly always accompanied by solar X-ray flares observed in the 0.1-0.8 nm band on the GOES X-ray Spectrometer (XRS), which are commonly used to forecast the occurrence of SEP events [7,8]. [2,3] took a novel approach to comparing GOES X-ray observations with SEP events by introducing the peak flare X-ray temperatures, based on the ratios of short 0.05-0.4 nm to long 0.1-0.8 nm wavelength bands. For a given range of peak 0.1-0.8 nm flare fluxes, the SEP events were preferentially associated with flares of lower peak temperatures.

Recently [1] revisited the [2,3] approach using a selection of all  $> M3$  X-ray flares with known source locations from 1998 to 2016. Rather than flare temperatures, [1] used simply the background-corrected peak flare ratios  $R$  of short 0.05-0.4 nm to long 0.1-0.8 nm versus the 0.1-0.8 nm peak intensities to sort out flare groups with (1) no associated SEP event; (2) a small (1.2-9.9 pfu) event; (3) a NOAA ( $\geq 10$  pfu) event; or (4) a  $\geq 300$  pfu event. The flares were divided into eastern and western hemisphere groups and plotted separately as shown in the left panels of Figure 1. [1] used the statistical t-test for three selected bins of peak-flux ratios to show low probabilities  $P$  of common populations, implying clear separations between the SEP and non-SEP groups based on flare peak X-ray ratios.

The introduction of peak-flux ratios adds information to any X-ray flare-based scheme to forecast SEP events, but it challenges our understanding of the physics behind the basic result of Figure 1. The current paradigm of SEP origins in CME-driven shocks is validated by the many results of good correlations between SEP peak intensities and associated CME speeds [4,5]. The question now is how lower-temperature X-ray flares are physically connected with the faster CMEs needed for SEP production. [1] pointed out that a global analysis by [9] led to a scaling law of  $V_{cme} \sim T_e^{0.5}$ , where  $V_{cme}$  is the CME speed and  $T_e$  is the X-ray flare temperature, a result seemingly in conflict with our results. The statistical correlation between X-ray flare peak fluxes and associated CME speeds  $V_{cme}$  [10,11,12,13] shows a clear connection between flares and CMEs, but any role for flare temperatures is not included in those correlations. Accepting the CME-shock paradigm for SEP events, the clear implication of Figure 1 is that a similar plot format discriminating among (1) faster SEP-producing CMEs; (2) slower non-SEP producing CMEs; and (3) no CMEs should yield a result similar to that with SEP and non-SEP events.

## 2. Data Analysis

Our goal is to determine whether the X-ray ratio plot format of Figure 1 also sorts CME speeds as it does SEP events. We begin with the same [1] list of all GOES  $> M3$  flares with known flare locations from 1998 to 2016. There were 433 flares without and 75 flares with  $\geq 10$  pfu SEP events in that list. We changed the flare locations of four events and added an X3.1 flare on 24 October 2014 to make a total of 509 flare events. As in [1] we consider separately the eastern and western hemisphere flares. The timing and location of each flare was compared with CMEs reported on the *SOHO/LASCO* web site ([https://cdaw.gsfc.nasa.gov/CME\\_list/index.html](https://cdaw.gsfc.nasa.gov/CME_list/index.html)) to determine the CME association, if any, for each flare. LASCO data gaps during 52 flares limited the comparisons to a

total of 457 cases. There were 100 flares with no associated CMEs. For each of the remaining 357 associated CMEs we listed the reported linear speed  $V_{cme}$  and width  $W$ .

In the right panels of Figure 1 we plot the 457 CME associations using the same X-ray flare format, now dividing the CME associations into three groups of (1) no, (2) slow ( $V_{cme} < 1000 \text{ km s}^{-1}$ ), and (3) fast ( $V_{cme} \geq 1000 \text{ km s}^{-1}$ ) CMEs. The fast CMEs lie preferentially in the low range of the R ratios. For the CME speed groups we find only modest ( $P \leq 0.4$ ) values comparing the no-CME with slow-CME groups, but much lower ( $P < .05$  for all but one bin) values distinguishing the slow and fast CME groups. This result validates the suspected reason for the SEP and no-SEP separation of Figure 1, that the SEP events result from a matching trend of no CME, to slow, to fast CMEs with progressively lower ratios R, which are taken as measures of peak X-ray flare temperatures.

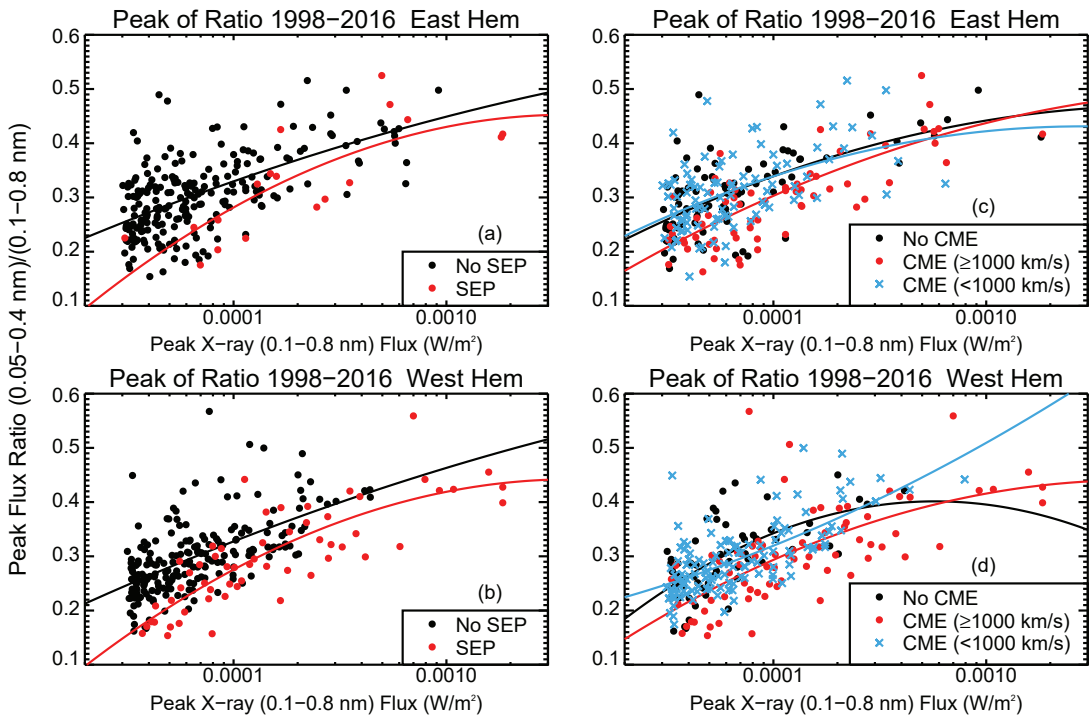


**Figure 1:** Left panels: Modified version of Figure 5 of [1], following the original format of [3]. Top panel: Peak flare X-ray flux ratios versus 0.1-0.8 nm peak fluxes for NOAA flares in the eastern hemisphere. Solid lines are polynomial quadratic best fits. Right panels: Peak X-ray flux ratios versus maximum 0.1-0.8 nm flare fluxes for three classes of  $V_{cme}$  associations. Solid lines are least-squares quadratic fits to color-matched symbols. Top and bottom panels: eastern and western hemisphere flares.

We now ask how the R ratios play a role in statistical correlations between X-ray flare peak fluxes and associated CME speeds found in [10,11,12,13]. Figure 2 shows a log-log plot of peak X-ray flare flux versus  $V_{cme}$  for flares in each hemisphere, again separated into three bands of R. Flares with no CMEs are plotted at  $\log V_{cme} = 2.0$ . The largest associated X-ray flare peaks tend to have the highest average ratios R, as noted in [1]. The appropriate interpretation here is that if hot flares are associated with a particular range of  $V_{cme}$ , they must also be large flares. Somewhat

counter-intuitively, cool flares in the same  $V_{cme}$  range have clearly lower peak fluxes. The t-test scores of pairs of different R groups, sorted into three bins of log CME speed, show those pairs to be clearly separated, with all  $P < 6 \text{ E-}4$ , and the Pearson CCs  $r$  for each peak-ratio group, which are largest for the highest R groups, are shown in the upper right of the Figure 2 left panels. The average of the three CME-associated group numbers in the eastern and western hemisphere are 53 and 66 events, respectively, so all  $r$  values of the left panels are significant at the 5% level.

CME widths  $W$ , as well as speeds  $V_{cme}$ , have been weakly correlated with SEP peak intensities [14,15,16], and we now look for a relation between the X-ray flare ratios  $R$  and associated CME widths  $W$ . The right panels of Figure 2 show plots of  $W$  versus log  $V_{cme}$  for the three R bands. First, we find correlations between  $W$  and log  $V_{cme}$  for all R bands significant at  $P < 0.1\%$ . The main question now is whether, in a given range of log  $V_{cme}$ , the widths  $W$  are enhanced in any R band. Looking back at Figure 1, we found that in each R band there were separations between SEP and non-SEP events, as well as between non-CMEs, slow CMEs, and fast CMEs. The CME speeds  $V_{cme}$  were the presumed explanation for the occurrence or absence of SEP events, but CME widths may also be part of the explanation. If so, we could expect that for a given range of log  $V_{cme}$  there is also a separation of populations of  $W$  based on their associated R values. The t-test values between the different R populations are low for both hemispheres, indicating no evidence that CME widths  $W$  are distinguished by their R values. The conclusion is that variation of flare R values is associated with variations in  $V_{cme}$ , but not in  $W$ , and that only the  $V_{cme}$  variations explain the separation of SEP from non-SEP events.

Flare durations may also be a factor in the final speeds of associated CMEs [17], with longer durations possibly indicating longer energy release times for driving CMEs to faster speeds  $V_{cme}$ . We can use the NOAA flare duration times  $\Delta T$  from onset to half peak value [18] as a parametric indication of a possible contributing factor to the separation of SEP and non-SEP flares. We look directly at the association between flare durations  $\Delta T$  and CME speeds  $V_{cme}$  in the left panels of Figure 3, with flares sorted between M and X-classes. The non-CME flares are plotted at log  $V_{cme} = 2.0$ . There is considerable scatter of the data points, but we find significant Pearson CCs ( $r \approx 0.4$ ) between flare  $\Delta T$  and log  $V_{cme}$  for both hemispheres and flare magnitude classes.

If, for a given flare peak flux, both lower peak flux ratios  $R$  and longer flare time durations  $\Delta T$  are associated with faster CMEs, as implied by Figures 1 (right panels) and 3 (left panels), then  $\Delta T$  should scale inversely with  $R$ . We confirm this expectation, although with a considerable scatter of points, in Figure 3 (right panels). This result suggests that one could repeat the [2,3] analysis of SEP versus non-SEP events by plotting flare  $\Delta T$  versus flare peak flux to find that for a given flare peak flux, SEP events are preferentially selected by longer  $\Delta T$ . How well this separation of SEP from non-SEP events works will probably depend critically on how well  $\Delta T$  is defined [19]. The end time definition would have to be better than using the current use of half-peak intensity time, but high backgrounds and subsequent flares make that determination difficult in full-Sun detectors.

Still unexplained by a simple conceptual model is why we find faster CMEs correlated with X-ray flares of either lower  $R$  or possibly longer  $\Delta T$ . A comprehensive analysis of 399 M and X GOES flares by [9] found a scaling law of  $V_{cme} \sim T_e^{0.5}$ , based on an assumed equipartition between CME kinetic energy and flare thermal energy. That result is inconsistent with Figure 2 (left panels) and with a qualitative explanation of [20] that CME activity removes energy from the source region, resulting in less energy available for flares, as indicated by lower peak flare

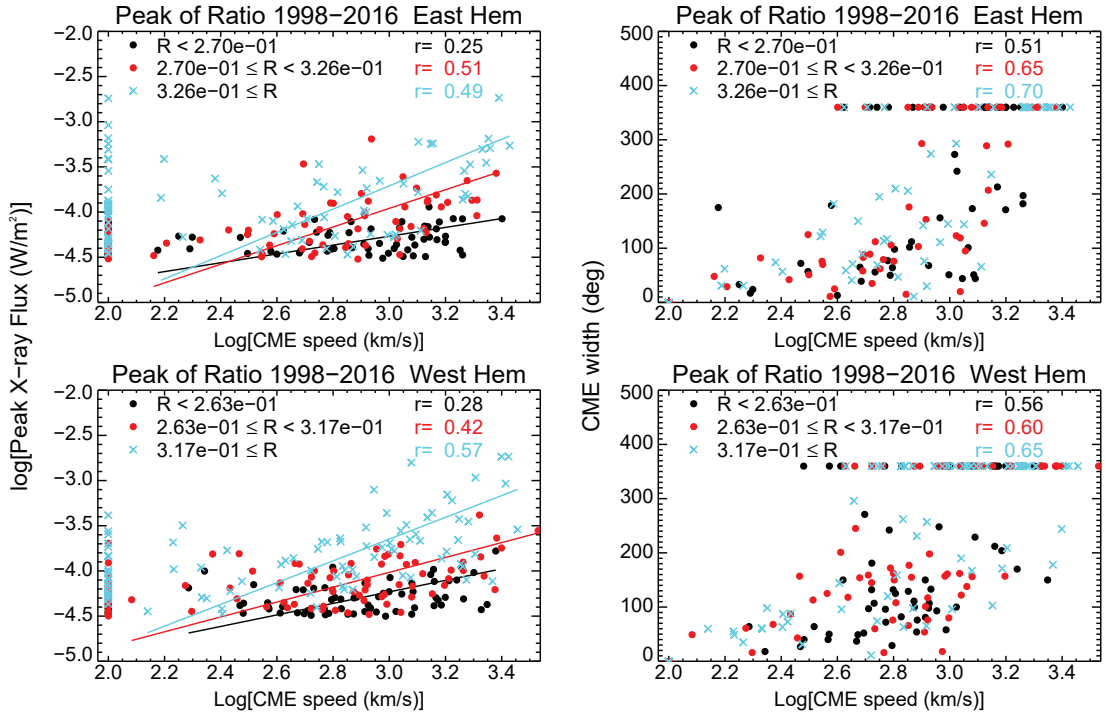


**Figure 2:** Left panels: Log of peak flare X-ray flux versus log of associated  $V_{\text{cme}}$  for three groups of peak X-ray flux ratios  $R$ . X-ray flares with no associated CMEs are plotted at  $\log V_{\text{cme}} = 2.0$ . Flares with associated CMEs are divided into three  $R$  groups of approximately equal sizes. Matching color-coded lines are linear least-squares best fits, with Pearson CCs  $r$  indicated in the top right of each panel. Right panels: CME width  $W$  versus log of  $V_{\text{cme}}$  for all X-ray flares with CME associations. Three  $R$  groups are approximately equal in size. Color-coded Pearson CCs  $r$  are shown for each  $R$  group in each panel. Points at  $W = 360^\circ$  are full-halo CMEs. Top and bottom panels: eastern and western hemisphere flares.

temperatures. We believe that Figure 4, now combining flares of both hemispheres, may resolve this observational paradox. In accordance with [9], there is a general weak correlation between  $V_{\text{cme}}$  and  $R$ , indicated by the linear best-fit solid line. However, if we consider only specific ranges of selected peak flare fluxes, shown by the three color-coded groups, then we find negative correlations between  $V_{\text{cme}}$  and  $R$ , as expected in the scheme of [20]. Thus, the validity of each energy scaling depends on whether the peak flux is held constant or allowed to be a free parameter. The result provides input for, but does not give a clear idea, of a simple model for energy scaling between flares and associated CMEs.

### 3. Discussion

Our earlier work [1] updated the [2,3] result showing that for a given X-ray flare peak flux, SEP events were associated preferentially with lower ratios  $R$ , indicative of cooler X-ray flares (Figure 1). We speculated that the physical reason for this result was that cooler flares were associated with the faster CMEs required to drive the shocks producing SEP events. Starting with our modified list of  $> M3$  flares, we searched the CDAW list for associated LASCO CMEs. Unlike the SEP

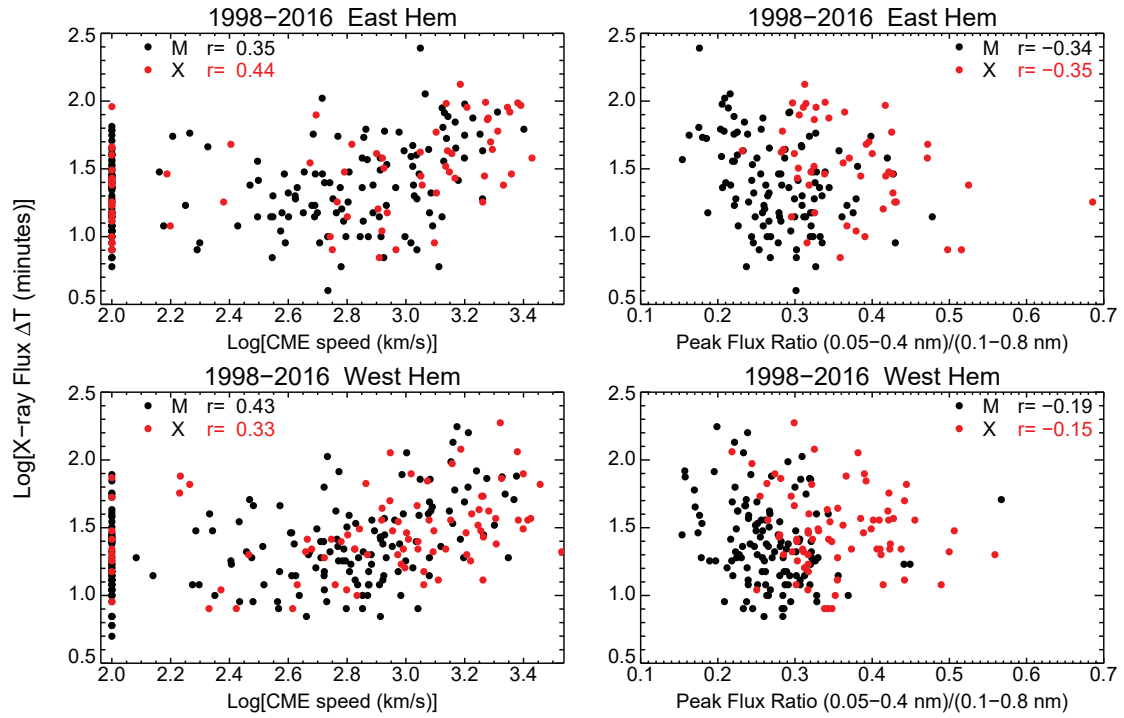


**Figure 3:** Left panels: Log X-ray flare duration  $\Delta T$  versus log of associated  $V_{cme}$ . Flares are differentiated between M and X-classes, and flares with no CME associations are plotted at log CME speed = 2.0. Color-matching Pearson CCs are given at the top of each panel for each flare group. Right panels: Log X-ray flare duration  $\Delta T$  versus flare peak-flux R for M and X flares. Top panel and bottom panels: eastern and western hemisphere flares.

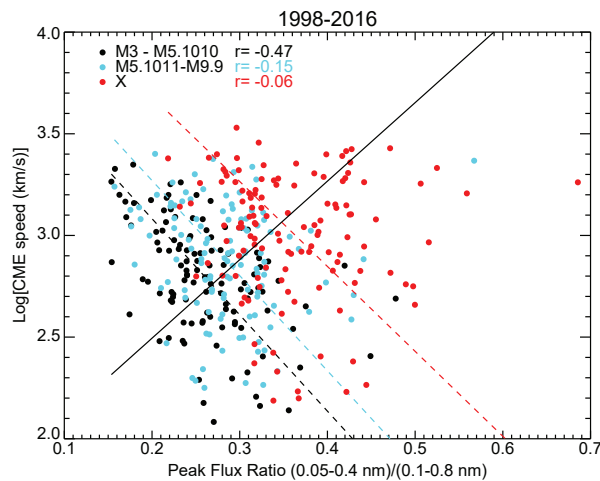


**Figure 4:** Log  $V_{cme}$  versus flare peak-flux R for three flare peak flux ranges of M and X flares and combined eastern and western hemispheres. There is a weak positive correlation for the combined flares (solid line), but negative correlations (dashed lines) for each of the three groups taken separately.

event associations with a bias for western hemisphere flare sources, the CME associations in each hemisphere should be similar and provide a consistency check on any single hemisphere result. First we find (Figure 1) that flares of a given peak X-ray flux without CMEs are somewhat hotter (higher  $R$ ) than those with slow ( $< 1000 \text{ km s}^{-1}$ ) CMEs. This result was found earlier [20] with a smaller data set of 69 flares. They speculated that the occurrence of a CME means that less energy goes into heating the associated flare. Perhaps consistent with that view, we find a more significant separation between the groups of slow ( $V_{\text{cme}} < 1000 \text{ km s}^{-1}$ ) and fast ( $\geq 1000 \text{ km s}^{-1}$ ) CMEs, where the latter group are known to have higher associations with SEP events.

We explored the role of the ratios  $R$  in the general correlation between X-ray peak flare fluxes and associated CME  $V_{\text{cme}}$ . The result (Figure 2) is that within that correlation there are strong separations by  $R$ , showing that within a given range of CME speeds the associated cooler (lower  $R$ ) flares have lower peak X-ray fluxes and the hotter have higher peak X-ray fluxes. CME widths  $W$  are correlated with speeds  $V_{\text{cme}}$  (Figure 2), but  $R$  does not define any significant group separations.

As our last parametric consideration, we looked at X-ray flare durations  $\Delta T$ , using the available SWPC definition of time from onset to half peak flux. A direct comparison of flare  $\Delta T$  versus  $\log V_{\text{cme}}$  (Figure 3) shows very significant correlations, which are independent of flare class. To complete the statistical comparison among  $\Delta T$ ,  $V_{\text{cme}}$ , and  $R$ , we find in Figure 4 modest inverse correlations between  $\Delta T$  and  $R$ , where the separation between M and X flares shows the well known (e.g., [21]) trend toward larger  $R$  values for larger peak flare fluxes. With a more accurate definition of  $\Delta T$  we might expect even higher correlations in Figure 3.

We can conclude not only that SEP events are associated with faster ( $V_{\text{cme}} \geq 1000 \text{ km s}^{-1}$ ) CMEs, but that the associated X-ray flares have lower peak temperatures (smaller  $R$ ) and longer  $\Delta T$  than non-SEP events. Although SEP intensities are correlated with CME widths  $W$ , we find that the X-ray parameters of  $R$  and  $\Delta T$  have no relation to  $W$ .

The basic question addressed in this work is whether the correlation of SEP events with X-ray flares of lower  $R$  can be attributed to a similar correlation of faster CMEs with flares of lower  $R$ . The answer is clearly yes, and we further found that X-ray flare ratios  $R$  serve to spread the correlation between X-ray flare peak fluxes and  $V_{\text{cme}}$  into bands from low  $R$  and low peak flux to high  $R$  and high peak flux for any range of  $V_{\text{cme}}$  (Figure 2). Finally, we find that flares with low  $R$  are also correlated with longer  $\Delta T$  (Figure 3), where the  $\Delta T$  values are taken only to the half peak intensities, rather than to near pre-flare backgrounds which might yield better correlations [19].

*Acknowledgements* S. Kahler was funded by AFOSR Task 18RVCOR122. A. Ling was supported by AFRL contract FA9453-15-C-0050. We have made use of the LASCO CME catalog, which is generated and maintained at the CDAW Data Center by NASA and The Catholic University of America in cooperation with the Naval Research Laboratory. SOHO is a project of international cooperation between ESA and NASA.

## References

- [1] S.W. Kahler, S.W., and A.G. Ling, *Forecasting Solar Energetic Particle (SEP) events with Flare X-ray peak ratios*, *J. Space Weather Space Clim.*, **8**, (2018), A47.
- [2] H.A. Garcia, *Temperature and hard X-ray signatures for energetic proton events*, *Astrophys. J.*, **420**, (1994), 422.

- [3] H.A. Garcia, *Forecasting methods for occurrence and magnitude of proton storms with solar soft X rays*, *Space Weather*, **2**, (2004), S02002.
- [4] D.V. Reames, *The Two Sources of Solar Energetic Particles*, *Space Sci.Rev.*, **175**, 53-92, (2013).
- [5] D.V. Reames, *Solar Energetic Particles: A Modern Primer on Understanding Sources, Acceleration and Propagation*, Lecture Notes in Physics, 932. Springer International Publishing AG, (2017).
- [6] D.V. Reames, *Abundances, Ionization States, Temperatures, and FIP in Solar Energetic Particles*, *Space Sci.Rev.*, **214**, (2018), 61.
- [7] C.C. Balch, *Updated verification of the Space Weather Prediction Center's solar energetic particle prediction model*, *Space Weather*, **6**, (2008), S01001.
- [8] S.W. Kahler, E.W. Cliver, and A.G. Ling. *Validating the proton prediction system (PPS)*. *J. Atmos. Solar-Terr. Phys.*, **69**, (2007), 43.
- [9] M.J. Aschwanden, *Global Energetics of Solar Flares. VI. Refined Energetics of Coronal Mass Ejections*, *Astrophys. J.*, **847**:27, (2017).
- [10] S. Yashiro, and N. Gopalswamy, *Statistical relationship between solar flares and coronal mass ejections*, *Universal Heliophysical Processes, Proc. I.A.U.*, IAU Symp. **257**, (2008), 233.
- [11] C. Salas-Matamoros and K.-L. Klein, *On the Statistical Relationship Between CME Speed and Soft X-Ray Flux and Fluence of the Associated Flare*, *Solar Phys.*, **290**, (2015), 1337.
- [12] R. Miteva, K.-L. Klein, O. Malandraki, and G. Dorrian, *Solar Energetic Particle Events in the 23rd Solar Cycle: Interplanetary Magnetic Field Configuration and Statistical Relationship with Flares and CMEs*, *Solar Phys.*, **282**, (2013), 579.
- [13] G. Trottet, S. Samwel, K.-L. Klein, T. Dudok de Wit, and R. Miteva, *Statistical Evidence for Contributions of Flares and Coronal Mass Ejections to Major Solar Energetic Particle Events*, *Solar Phys.*, **290**, (2015), 819.
- [14] S.W. Kahler, J. Burkepile, and D. Reames, *Coronal/Interplanetary Factors Contributing to the Intensities of  $E > 20$  MeV Gradual Solar Energetic Particle Events*. *Proc. 26th ICRC.*, **6**, (1999), 248.
- [15] S.W. Kahler, and D.V. Reames, *Solar Energetic Particle Production by Coronal Mass Ejection-driven Shocks in Solar Fast-Wind Regions*, *Astrophys. J.*, **584**, (2003), 1063.
- [16] M. Dierckxsens, K. Tziotziou, S. Dalla, I. Patsou, M.S. Marsh, N.B. Crosby, O. Malandraki, and G. Tsiropoula, *Relationship between Solar Energetic Particles and Properties of Flares and CMEs: Statistical Analysis of Solar Cycle 23 Events*, *Sol. Phys.*, **290**, (2015), 841.
- [17] S.W. Kahler, N.R. Sheeley, Jr., and M. Liggett, *Coronal mass ejections and associated X-ray flare durations*, *Astrophys. J.*, **344**, (1989), 1026.
- [18] A. Veronig, M. Temmer, A. Hanslmeier, W. Otruba, and M. Messerotti, *Temporal aspects and frequency distributions of solar soft X-ray flares*, *Astron. Astrophys.*, **382**, (2002), 1070.
- [19] D.F. Ryan, M. Dominique, D. Seaton, K. Stegen, and A. White, *Effects of flare definitions on the statistics of derived flare distributions*, *Astron. Astrophys.*, **592**, (2016), A133.
- [20] H.R.M. Kay, L.K. Harra, S.A. Matthews, J.L. Culhane, and L.M. Green, *The soft X-ray characteristics of solar flares, both with and without associated CMEs*, *Astron. Astrophys.*, **400**, (2003), 779.
- [21] D.F. Ryan, R.O. Milligan, P.T. Gallagher, B.R. Dennis, A.K. Tolbert, R.A. Schwartz, and C.A. Young, *The thermal properties of solar flares over three solar cycles using GOES X-ray observations*, *Astrophys. J. Suppl.*, **202**, (2012), 11.